Carbohydrate Polymers 121 (2015) 10–17

Contents lists available at ScienceDirect

Carbohydrate Polymers

journal homepage: www.elsevier.com/locate/carbpol

Effect of net surface charge on physical properties of the cellulose nanoparticles and their efficacy for oral protein delivery

Yongbo Song, Lingyun Chen*

Department of Agricultural, Food and Nutritional Science, University of Alberta, Edmonton, T6G 2P5, Canada

ARTICLE INFO

Article history:
Received 17 August 2014
Received in revised form 5 December 2014
Accepted 21 December 2014
Available online 27 December 2014

Keywords:
Cellulose nanoparticles
Surface charge
Cellular uptake
Oral delivery
Protein carrier

ABSTRACT

Both net positively and negatively charged cellulose-based nanoparticles were prepared from oppositely charged carboxymethylcellulose (CMC) and quaternized cellulose (QC). Effect of surface charge on efficacy of cellulose nanoparticles for delivering both positively and negatively charged proteins was investigated. Lysozyme (LYS) and bovine serum albumin (BSA), which possess positive and negative charge at physiological pH respectively, were used as models. The results revealed that high encapsulation efficiency (67.7% and 85.1%) could be achieved when negatively charged protein was encapsulated in positively charged nanoparticles, or positively charged protein was encapsulated in negatively charged nanoparticles. Proteins encapsulated in optimal cellulose nanoparticles could be sustainably released and no obvious protein denaturation was detected. Both net positively and negatively charged nanoparticles exhibited low cytotoxicity due to cellulose's good biocompatibility. Not only net positively charged nanoparticles demonstrated high cellular uptake efficiency, but also net negatively charged nanoparticles showed somewhat efficient cellular uptake.

1. Introduction

Compared with other routes of administration, oral delivery still remains as the most favorable and preferred route for drugs administration (Ramineni, Cunningham, Dziubla, & Puleo, 2013; Win & Feng, 2005). The oral route has attractive advantages such as convenience, low costs, and high patient compliance, which can avoid injections and decrease risk of infection (Win & Feng, 2005). However, the oral protein drugs usually exhibit the low level of bioavailability (Chen et al., 2008). The major challenges include the poor protein absorption and internalization through the gastrointestinal epithelium, as well as the rapid hydrolytic and enzymatic protein degradation by the gastrointestinal fluids (Harush-Frenkel, Rozentur, Benita, & Altschuler, 2008; Sandri et al., 2007; Thanou et al., 2000).

In order to overcome the above obstacles and improve the gastrointestinal uptake of protein drugs, different delivery systems have been investigated (Sadeghi et al., 2008). An effective approach is to entrap proteins within polysaccharide nanoparticles, which could protect proteins from degradation in the gastrointestinal fluids and deliver them to the target sites for release, and improve their permeation across the gastrointestinal epithelium (des Rieux, Fievez, Garinot, Schneider, & Préat, 2006; Jadhav & Singhal, 2014; Li et al., 2011; Mo, Jiang, Di, Tai, & Gu, 2014; Pan et al., 2002). Polysaccharides are considered as highly safe, biocompatible, and biodegradable natural biomaterials. Moreover, most of polysaccharides have hydrophilic groups such as hydroxyl, carboxyl, and amino groups, which could form non-covalent bonds with biological tissues such as intestinal mucosa to facilitate protein drug absorption (Liu, Jiao, Wang, Zhou, & Zhang, 2008; Song, Zhou, Li, Guo, & Zhang, 2008).

Cellulose is one of the most widely used natural substances and has become one of the most important commercial biopolymeric raw materials (Song et al., 2011). Microcrystalline cellulose and cellulose derivatives, such as carboxymethyl cellulose (CMC), hydroxyethyl cellulose (HEC), hydroxypropyl cellulose (HPC), and hydroxypropylmethyl cellulose (HPMC), are recognized as the natural materials with good tolerance by the body (Mahmoud et al., 2010), and have been routinely used in medical and pharmaceutical applications such as controlled delivery systems (Kamel, Ali, Jahangir, Shah, & El-Gendy, 2008). In our previous works (Song, Zhou, & Chen, 2012; Song, Zhou, van Drunen Littel-van den Hurk, & Chen, 2014), the polyelectrolyte complex nanoparticles were prepared by mixing negatively charged carboxymethyl cellulose (CMC) and positively charged quaternized cellulose (QC) in an aqueous medium. The novel CMC–QC nanoparticles have been proven to be a promising delivery system of negatively charged proteins and DNA vaccines. The surface charge is very important for such systems,

* Corresponding author. Fax: +1 780 492 4265.
E-mail address: lingyun.chen@ualberta.ca (L. Chen).

http://dx.doi.org/10.1016/j.carbpol.2014.12.019
0144-8617/

involving an encapsulation efficacy, cytoxicity, and cellular uptake (Song et al., 2010). Thus it is hypothesized that CMC–QC nanoparticle surface charge can be modulated to encapsulate protein drugs of different isoelectric points (pI) and controlled release them into small intestine for improved absorption. The test of this hypothesis relies on a fundamental understanding of the protein delivery properties of cellulose nanoparticles as impacted by surface charge.

In this work, both the net negatively charged and positively charged CMC–QC nanoparticles were prepared by changing the ratio of anionic-to-cationic polymers. Two proteins, lysozyme (LYS, pI 11.4) and bovine serum albumin (BSA, pI 4.8), with opposite charges in physical condition were selected as models. It was expected that these two types of proteins could be encapsulated in both negatively charged and positively charged CMC–QC nanoparticles. The challenge was to encapsulate the cationic protein LYS molecule into the positively charged nanoparticles, while encapsulate the anionic protein BSA molecule into the negatively charged nanoparticles. To overcome this challenge, we attempted to mask the positively charged LYS by complex LYS with the polyanion CMC, while masking the negatively charged BSA by complex BSA with the polycation QC. The effects of surface charge on encapsulation efficacy, release, cytoxicity, and cellular uptake of cellulose nanoparticles were systematically investigated. These studies provided the important information of scientific value for designing the cellulose-based nanoparticles to be used as the delivery vectors efficiently and specifically.

2. Experimental methods

2.1. Materials

Wood cellulose (spruce bleached sulphate pulp) was kindly provided by Alberta-Pacific Forest Industries Inc. (Alberta, Canada), and the molecular weight was determined by viscometry in LiOH/urea aqueous solution to be 40.5×10^4 g/mol (Song et al., 2012). 3-[4,5-dimethylthiazol-2-yl]-2,5-diphenyltetrazolium bromide (MTT), Fetal bovine serum (FBS), and Minimal Essential Medium (MEM) were purchased from Invitrogen Corp. (CA, USA). Caco-2 cells were purchased from American Type Culture Collection (ATCC, VA, USA). Sodium monochloroacetate, 3-chloro-2-hydroxypropyltrimethylammonium chloride (CHPTAC), LYS, BSA, Coumarin-6 (COUM-6), 4′,6-diamidino-2-phenylindole (DAPI), and Alexa Fluor® 594 conjugate of Concanavalin A were purchased from Sigma-Aldrich (MO, USA). Other reagents were of analytical grade and used without further purification.

QC and CMC were prepared according to previous work (Song et al., 2012). Briefly, 50 g CHPTAC (60 wt% aq.) or 25 g solid sodium monochloroacetate was added gradually into 100 g of wood cellulose solution (1 wt% in LiOH/urea aq.), respectively, and then the mixture was stirred vigorously. The quaternization reaction was kept at 25 °C for 24 h, while the carboxymethylation reaction was kept at 55 °C for 5 h. The reaction products were dialyzed against distilled water, and freeze-dried to obtain the water-soluble QC and CMC samples.

2.2. Preparation and characterization of CMC–QC nanoparticles

LYS-encapsulated CMC–QC nanoparticles were prepared by the following method: 10 mL LYS aqueous solutions were mixed with 10 mL CMC aqueous solutions, then 10 mL QC aqueous solutions was added and followed by vigorous vortex for 30 s. As for BSA, 10 mL BSA aqueous solutions were mixed with 10 mL QC aqueous solutions, then 10 mL CMC aqueous solutions was added and mixed by vigorous vortex. Detailed preparation conditions are summarized in Table 1. The formed suspensions were kept for 30 min at room temperature before further use or characterization.

The zeta potential was measured using Zetasizer Nano-ZS ZEN1600 (Malven Instruments, UK) at 25 °C. The particle size was measured based on dynamic laser scattering (DLS, Malven Instruments, UK). The morphology of the protein-encapsulated CMC–QC nanoparticles was observed using a transmission electron microscope (TEM, Philips Morgagni 268, FEI Company, Netherlands). Freshly prepared samples were placed on a copper grid covered with Formvar film. After the deposition, the aqueous solution was blotted away with a strip of filter paper, and then examined at 80 kV.

2.3. Protein encapsulation and in vitro release

The protein encapsulation efficiency (EE) and loading capacity (LC) of CMC–QC nanoparticles was determined by isolating the nanoparticles from suspension by centrifugation at 20,000 rpm for 30 min. The concentration of remaining free protein in the clear supernatant was determined by micro-BCA protein assay. Absorbance was measured by a microplate reader (GENios, Tecan, Männedorf, Switzerland). The standard curves for proteins concentration was created using known concentrations of proteins. EE and LC were calculated as follows:

$$\text{EE}\ \ (\%) = 100 \times (W_0 - W_f)/W_0$$

$$\text{LC}\ \ (\%) = 100 \times (W_0 - W_f)/W_N$$

where, W_0 was the total weight of protein added, W_N was the total weight of nanoparticles, and W_f was the weight of free protein remained in the supernatant.

In vitro protein release profiles from CMC–QC nanoparticles were determined as follows: 5 mg lyophilized protein-loaded nanoparticles were dispersed into 20 mL HCl buffer at pH 1.2 (simulated gastric fluid), then incubated on a shaking water bath at 37 °C, 100 rpm for 2 h. At appropriate intervals, 0.4 mL supernatant was taken, separated from nanoparticles by centrifugation (20,000 rpm, 30 min) for protein determination and replaced by fresh medium. After 2 h, the nanoparticles were transferred to 20 mL phosphate buffer at pH 6.8 (simulated intestinal fluid) and incubated at 37 °C for additional 4 h. At appropriate intervals, 0.4 mL supernatant was taken, separated from nanoparticles by centrifugation (20,000 rpm, 30 min) for protein determination and replaced by fresh medium. The concentration of released protein was determined by micro-BCA protein assay.

2.4. Bioactivity of released lysozyme

The relative bioactivity of released lysozyme was determined using the decrease in optical density at 450 nm of a *Micrococcus luteus* suspension. Briefly, *M. luteus* was suspended into phosphate buffer solution (66 mM PBS, pH 6.15), and then diluted to obtain an absorbance (at 450 nm) between 0.2 and 0.6. Then 0.1 mL aliquot of appropriately diluted lysozyme sample was mixed with 2.5 mL prepared *M. luteus* suspension in a quartz cell, which was then immediately placed into a spectrophotometer. The rate of decrease of absorbance at 450 nm was monitored by a microplate reader (GENios, Tecan, Männedorf, Switzerland) during a total period of 2 min at 25 °C. The relative bioactivity of lysozyme was calculated from the linear slope of the curve (absorbance versus time) according to the technique described by van de Weert et al. (van de Weert, Hoechstetter, Hennink, & Crommelin, 2000).

Table 1
The preparation conditions, zeta potential, particle size, encapsulation efficiency (EE), and loading capacity (LC) of protein-encapsulated CMC–QC nanoparticles.

Sample	CMC (mg)	QC (mg)	LYS/BSA (mg)	ζ (mV)	Size (nm)	PDI	EE (%)	LC (%)
LYS−	10	2	20	−25.1 ± 0.3	216.8 ± 2.6	0.118 ± 0.009	85.1 ± 0.1	60.8 ± 2.2
LYS+	10	15	20	+25.4 ± 0.5	225.4 ± 5.9	0.254 ± 0.021	65.4 ± 0.2	36.2 ± 0.9
BSA+	2	10	20	+26.8 ± 0.8	208.5 ± 5.2	0.175 ± 0.015	67.7 ± 0.3	54.2 ± 2.3
BSA−	20	10	20	−26.4 ± 0.5	206.0 ± 4.4	0.186 ± 0.008	42.1 ± 0.1	23.1 ± 1.1

2.5. In vitro cytotoxicity assay

The cytotoxicity of protein-encapsulated CMC–QC nanoparticles was examined by MTT assay. Caco-2 cells were seeded in 96-well plates at 6000 cells/well and cultured in 150 μL Minimal Essential Medium (MEM) at 37 °C for 24 h. The medium in each well was then replaced with protein-encapsulated nanoparticles solutions (5–20% v/v in 150 μL serum-free MEM). Cell viability was tested 6 h later. 20 μL aliquots of MTT solution (5 mg/mL in PBS) were added to each well and the plates were incubated at 37 °C for 4 h, followed by removal of the media and addition of 150 μL DMSO to each well. The absorbance was measured at 570 nm using a microplate reader (GENios, Tecan, Männedorf, Switzerland), and relative cell viability was calculated.

2.6. In vitro cellular uptake

Caco-2 cells (5×10^4 cells/well) were seeded into the glass bottom microwell dish (No. 1.5 coverglass, MatTek Corp., MA, USA), and allowed to be cultured at 37 °C for 24 h. Protein was labeled with COUM-6 as follows: 1 mL COUM-6 solution (5 mg/mL in DMSO) was added to 100 g protein aqueous solution (1 wt%), the solution was stirred for 2 h and dialyzed extensively against distilled water in dark, and then freeze-dried. Freshly prepared COUM-6 labeled protein-encapsulated CMC–QC nanoparticles (15% v/v in 2 mL serum-free MEM) were added into the cells and incubated for 6 h. For confocal laser scanning microscopy, cells were fixed with an ice-cold solution of 3.7% formaldehyde in PBS (0.01 M, pH 7.4) for 30 min, and then washed three times with PBS. In order to observe the nanoparticles uptake in the cells, cell nuclei were stained with DAPI (1 μg/mL in PBS), cell apical membranes were stained with Alexa Fluor® 594 conjugate of Concanavalin A (5 μg/mL in PBS). The dish was kept in dark for 1 h. Cells were observed with a CLSM 510 Meta confocal laser scanning microscope (Carl Zeiss, Jena, Germany). The fluorescent images of cells were analyzed simultaneously at wavelengths of 405, 488, and 561 nm. Images were processed with ZEN 2009 LE software. An oil immersion objective (40×) was used. For flow cytometry, cells were removed from the wells using cold EDTA (0.6 mM in PBS), transferred to tubes and analyzed directly (FACSCalibur, BD Biosciences, San Jose, CA, USA).

2.7. Statistical analysis

All samples were prepared and tested in triplicate or more. Data were presented as mean ± standard deviation (SD). The statistical significance of differences between groups was determined by Student–Newman–Keuls (SNK) test. The differences were considered significant for $^{*}P < 0.05$.

3. Results and discussion

3.1. Formation of CMC–QC nanoparticles

The formation of protein-encapsulated CMC–QC nanoparticles was through the electrostatic interaction between the negatively charged CMC and the positively charged QC, as well as the charged proteins (Scheme 1). Take positively charged LYS for example, when LYS aqueous solutions were mixed with CMC aqueous solutions, the electrostatic interaction occurred between the positively charged LYS and the negatively charged CMC, which formed the LYS–CMC complex. When QC aqueous solutions were added into LYS–CMC complex, the electrostatic attractions between CMC and QC caused CMC and QC macromolecular chains to curl up and form insoluble LYS-encapsulated CMC–QC nanoparticles (Song et al., 2012).

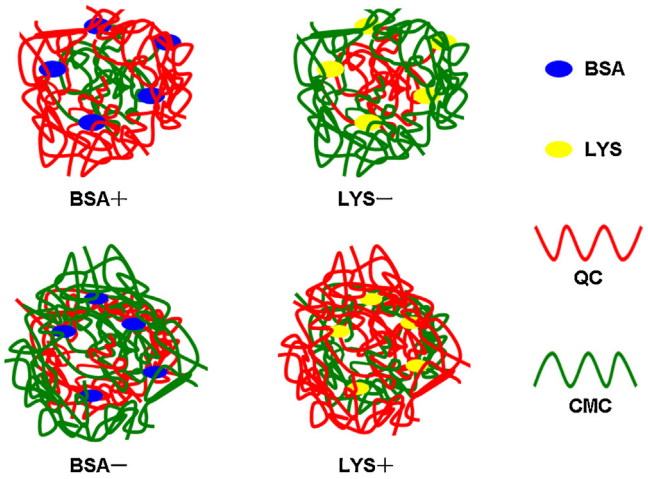

Scheme 1. Schematic representation of the formation of CMC–QC nanoparticles.+ means QC is excessive; while −means CMC is excessive.

The formation and properties of LYS-encapsulated CMC–QC nanoparticles depended on the charge ratio of anionic-to-cationic polymers (Song et al., 2012). When small amount of QC was added, COO^- on CMC chains was in excess, and negatively charged nanoparticles (LYS–) formed, where QC acted as the ionic cross-linking agent among multiple CMC molecular chains. By contrast, when excessive QC was added, $(CH_3)_3N^+$ on QC chains was in excess, then CMC acted as the ionic cross-linking agent and positively charged nanoparticles (LYS+) were formed (Boddohi, Moore, Johnson, & Kipper, 2009; Drogoz, David, Rochas, Domard, & Delair, 2007; Sæther, Holme, Maurstad, Smidsrød, & Stokke, 2008). While the charge ratio reached close to 1:1, the surface charge of nanoparticles was neutralized, which led to precipitates (Schatz, Domard, Viton, Pichot, & Delair, 2004). As for the negatively charged BSA, the situations were the same, except that BSA interacted with QC first and was followed by CMC addition. For better comparison, we chose both the positively and negatively charged protein-encapsulated CMC–QC nanoparticles with almost same particle size (~210 nm) and values (~±26 mV) of zeta potential (Table 1) for the further studies.

3.2. Morphology

The representative morphology of nanoparticles with both proteins was observed by transmission electron microscopy. As illustrated from Fig. 1, both two kinds of protein-encapsulated CMC–QC nanoparticles were approximately spherical and dispersed homogeneously. This homogeneous dispersal was due to

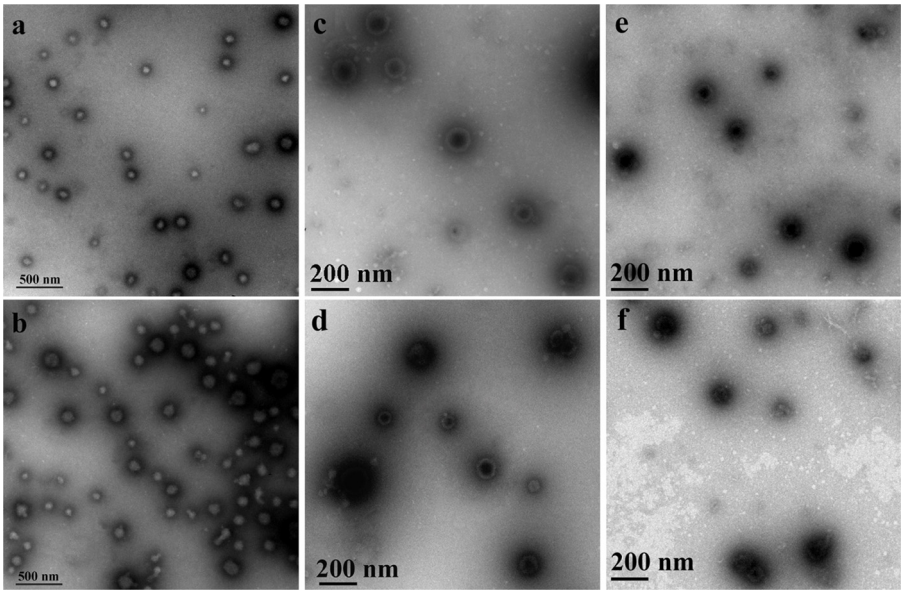

Fig. 1. TEM images of protein-encapsulated CMC–QC nanoparticles. (a) LYS−; (b) LYS+; (c) BSA+; (d) BSA−; (e) positively; and (f) negatively charged CMC–QC nanoparticles without proteins for comparison.

the electrostatic repulsions of the positive or negative charges on nanoparticle surfaces (Chen, Hu, Chen, Jiang, & Yang, 2005). The mean size of BSA-encapsulated CMC–QC nanoparticles was about 150 nm; and the mean size of LYS-encapsulated CMC–QC nanoparticles was about 155 nm. The mean sizes observed by TEM were slightly smaller than those measured from the dynamic laser scattering (Table 1). This may be explained by the hydration effect. The particle size measured by dynamic laser scattering is the hydrodynamic diameter in aqueous solutions, while it is that of dried nanoparticles when measured by TEM.

3.3. Proteins encapsulation and in vitro release

As shown in Table 1, the encapsulation efficiency (EE) and loading capacity (LC) of LYS in the negatively charged CMC–QC nanoparticles (LYS−) could reach 85.1% and 60.8%, respectively. While with the addition of more QC, positively charged nanoparticles (LYS+) were formed and EE and LC of LYS decreased to 65.4% and 36.2%, respectively. This decrease was because the excessive positively charged QC could compete with the positively charged LYS, which led to the decreased attraction between LYS and CMC. Subsequently more LYS was lost and then EE and LC decreased as a result (Cai, Bakowsky, Rytting, Schaper, & Kissel, 2008). Similarly for BSA, EE and LC of BSA in the positively charged nanoparticles (BSA+) was 67.7% and 54.2%, respectively. For the negatively charged nanoparticles (BSA−), the addition of excessive CMC could compete with the negatively charged BSA, and then the encapsulation efficiency decreased to 42.1% and 23.1%, respectively.

The in vitro release of LYS and BSA from CMC–QC nanoparticles under gastric followed by intestinal simulated pH conditions was investigated. As shown in Fig. 2, for all the studied nanoparticles, the initial burst release up to about 20% at pH 1.2 was observed in the first 0.5 h, followed by a plateau state. The initial burst release of proteins might be owing to protein release from the nanoparticle surface, due to the weak interaction forces between the polyelectrolytes and the protein (Yeo & Park, 2004). However, proteins encapsulated within the nanoparticle matrix faced an additional physical barrier. Further gastric protection against proteins release can be attributed to the more effective retention by a tight CMC network that forms at low pH (Sarmento et al., 2007). When transferred to pH 6.8 buffer simulating intestinal conditions, CMC swells

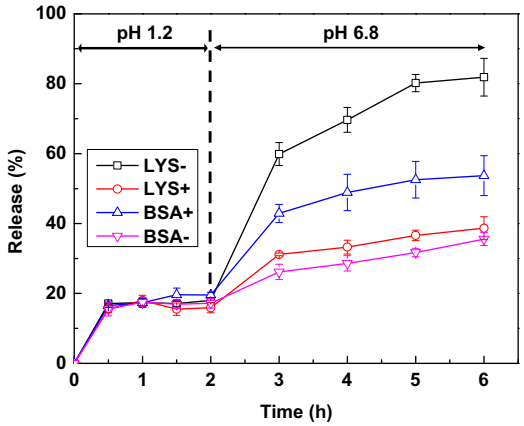

Fig. 2. The release profiles of proteins from CMC–QC nanoparticles in pH 1.2 simulated gastric fluid for 2 h followed by 4 h in pH 6.8 simulated intestinal fluid at 37 °C.

as it forms an ionic state, contributing to a higher amount of proteins release. In simulated intestinal conditions, the proteins were gradually released from inside of nanoparticles, resulting from the diffusion of protein and the swelling and erosion process of the cellulose nanoparticles matrix (Bouillot et al., 1999; Chen, Remondetto, Rouabhia, & Subirade, 2008). The encapsulated BSA was released to around 53.70% after 6 h from the positively charged nanoparticles (BSA+). The encapsulated LYS was released up to about 81.89% from the negatively charged nanoparticles (LYS−) until 6 h. As for BSA− nanoparticles and LYS+ nanoparticles, the proteins release (up to 6 h) was slower than the above two nanoparticles (BSA+ and LYS− nanoparticles). The percentage of protein released after 6 h from BSA− and LYS+ nanoparticles was 35.54% and 38.67%, respectively. The reason might be that the proteins were incorporated with more QC and CMC molecular chains (Scheme 1) in these two nanoparticles (BSA− and LYS+), and then the electrostatic interaction between incorporated proteins and CMC–QC nanoparticles matrix was stronger. These release results suggested that the proteins encapsulated in optimal CMC–QC nanoparticles could be sustained-released.

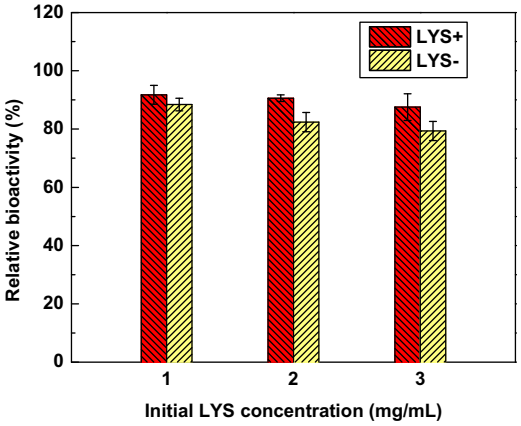

Fig. 3. The relative bioactivity (%) (with respect to the free enzyme) of LYS released from nanoparticles (6 h). CMC concentration was 1.0 mg/mL. QC concentration was 0.2 and 1.5 mg/mL. Data were measured by activity against *Micrococcus luteus*. The free LYS solution bioactivity was used as control (100%).

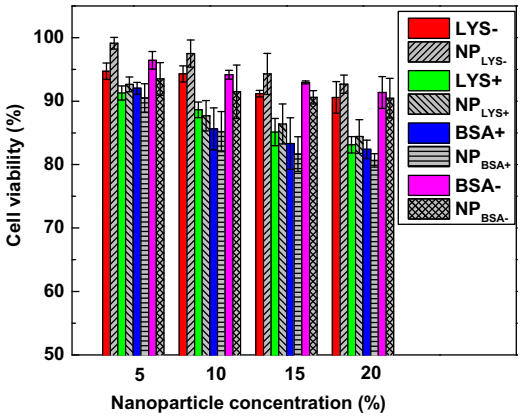

Fig. 4. Cell viability of Caco-2 cells in the presence of protein-encapsulated CMC–QC nanoparticles. Gray bars were the corresponding blank CMC–QC nanoparticles without proteins for comparison.

3.4. Bioactivity of protein released from nanoparticles

The preservation of protein bioactivity during the process of encapsulation and release remains a challenge. In order to verify that the CMC–QC nanoparticles preparation and release process do not denature the proteins, the bioactivity of released LYS was determined relative to that of free LYS. LYS with difference added concentration (1, 2, and 3 mg/mL) was chose as the examples. As shown in Fig. 3, no significant difference of bioactivity was observed for different added LYS concentrations ($P > 0.05$). For the negatively charged nanoparticles (LYS−), the bioactivity of LYS was determined to be from 79.35 to 88.43%. While for the positively charged nanoparticles (LYS+), the processes of encapsulation and release had only a little effect on the relative bioactivity of LYS. The full bioactivity of LYS was preserved throughout (87.53–91.75%), which confirmed that no obvious LYS denaturation was detected during the process of encapsulation or release. This protein-encapsulated nanoparticles preparation procedure was convenient under extremely mild aqueous conditions at room temperature, which protected the sensitive proteins from the attack of organic solvent and high temperature. Furthermore, proteins was encapsulated inside the biocompatible cellulose nanoparticles, which could supply the better proteins protection and reduce the proteins denaturation, so the native LYS structure still maintained in the capsulation system and could be released intact in the physical buffer. Accordingly, this may be a facile and feasible method for preparing protein-loaded nanoparticles, while preserving the protein bioactivity during the process of encapsulation and release.

3.5. In vitro cytotoxicity assay

The cytotoxicity of LYS and BSA-encapsulated CMC–QC nanoparticles was evaluated in Caco-2 cells by MTT assay. The corresponding blank CMC–QC nanoparticles without proteins were studied for comparison. The effect of the nanoparticles concentration and surface charges on the proliferation of Caco-2 cells was studied and shown in Fig. 4. It could be seen that the surface charge of CMC–QC nanoparticles was an important factor in determining the cytotoxicity. As we known, the positive surface charge could damage the cellular membranes, and may cause toxicity mediated through membrane effects (Garnett & Kallinteri, 2006). Herein it is interesting to notice that the positively charged nanoparticles showed low toxicity (cell viability more than 82.41%), which probably because of the cellulose biocompatibility. Moreover, the negatively charged nanoparticles didn't exhibit obvious cytotoxicity (cell viability more than 90.59%) due to the negative surface charge. Cell viability assays indicated that CMC–QC nanoparticles exhibit low toxicity and could be safe for oral protein delivery.

3.6. Cellular uptake

3.6.1. Confocal laser scanning microscopy

The cellular uptake profile will reflect the delivery efficiency of the carriers (Yue et al., 2011). To study the effect of surface charge on cellular uptake of CMC–QC nanoparticles, Caco-2 cells incubated with the protein-encapsulated nanoparticles were observed by confocal laser scanning microscopy. The proteins were stained green using COUM-6, the cell nuclei were stained blue using DAPI, and the cell membranes were stained red using the Alexa Fluor® 594 conjugate of Concanavalin A. The association of COUM-6 itself with cells was firstly examined, and no green fluorescent signal was detected (data not shown), indicating that this probe alone was not internalized in 6 h (Zhang, Field, Vine, & Chen, 2014). By contrast as illustrated obviously in Fig. 5, positively charged nanoparticles encapsulating both protein model drugs (BSA+ and LYS+) exhibited efficient cellular uptake by Caco-2 cells as green COUM-6 labeled proteins were accumulated in the cytoplasm of Caco-2 cells. The cationic surface charge and the nano-scale size of protein-encapsulated CMC–QC nanoparticles would have facilitated cellular uptake because such nanoparticles could electrostatically interact with the negatively charged cell membrane, and then were internalized likely into the cells through endocytosis (Mao, Zhou, & Gao, 2013).

Compared with the positively charged nanoparticles (BSA+ and LYS+), there was much less cellular uptake of the negatively charged protein-encapsulated nanoparticles (BSA− and LYS−). Such behavior could be the result of electrostatic repulsive forces between the negatively charged nanoparticles and the negatively charged cellular membrane (Mahmoud et al., 2010).

3.6.2. Flow cytometry

To further quantify the cellular internalization of CMC–QC nanoparticles by Caco-2 cells, the fluorescence intensity of COUM-6 labeled protein-encapsulated nanoparticles was also assessed by flow cytometry (Fig. 6). COUM-6 alone and COUM-6 labeled proteins were used for comparison. The internalization of

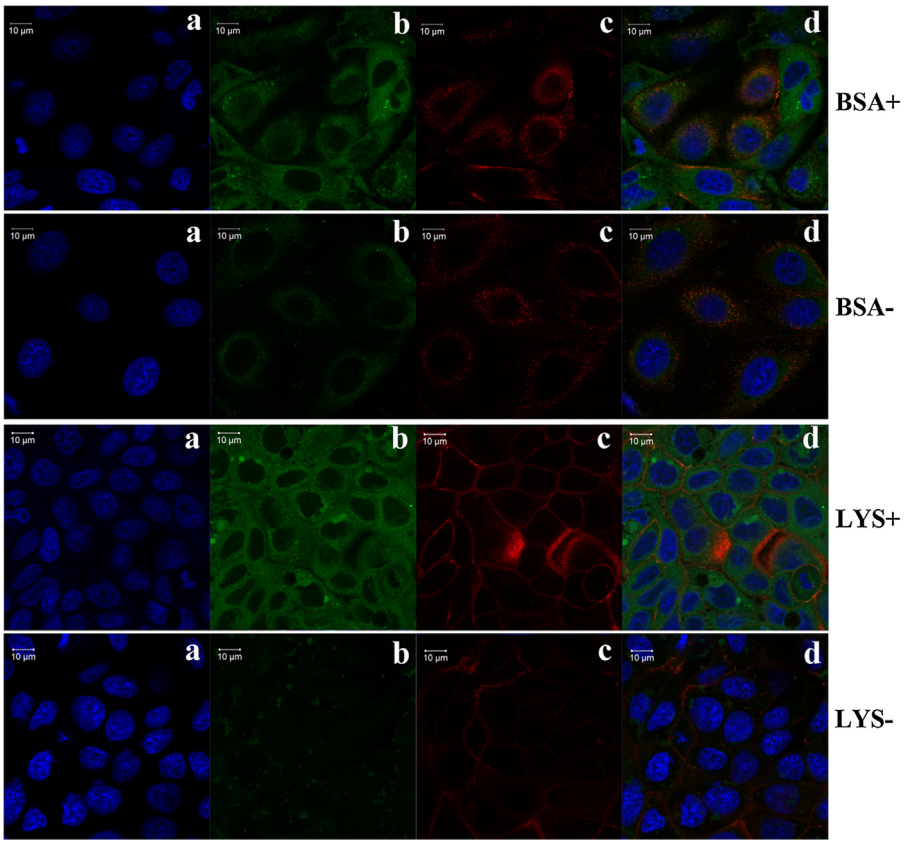

Fig. 5. Confocal microscopic images of Caco-2 cells incubated with the protein-encapsulated CMC–QC nanoparticles. (a) Fluorescence blue channel of cell nuclei, (b) fluorescence green channel of protein, (c) fluorescence red channel of cell membranes, and (d) overlapped image (For interpretation of the references to colour in this figure legend, the reader is referred to the web version of this article.).

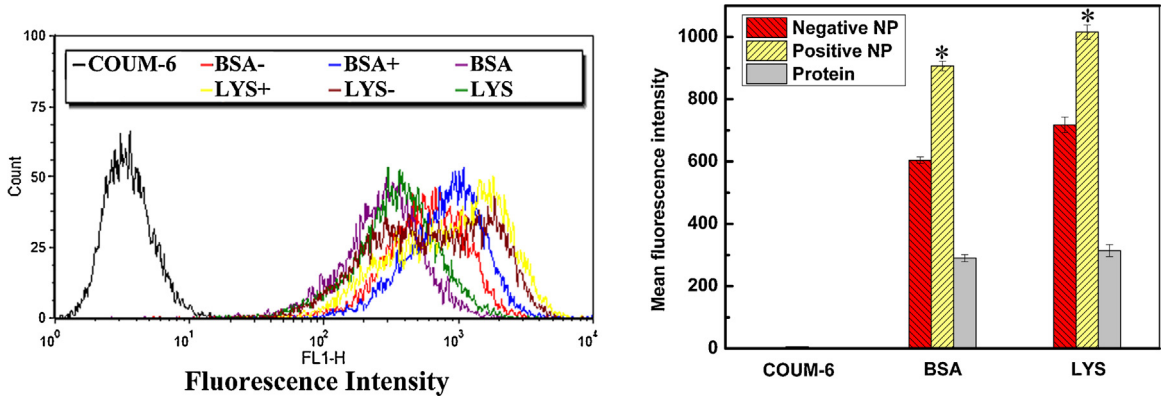

Fig. 6. Flow cytometry analysis of fluorescence intensity of COUM-6, COUM-6 labeled proteins, and protein-encapsulated CMC–QC nanoparticles in Caco-2 cells. $^{*}P < 0.05$ compared with the free protein and negatively charged nanoparticles.

nanoparticles into Caco-2 cells was assessed by mean fluorescence intensity (MFI) of nanoparticles inside Caco-2 cells. A higher MFI means more nanoparticles internalization. As shown, cellular internalization of free proteins was low due to their big size, which makes the low permeability. When protein was loaded in compact cellulose nanoparticles, it is easier for cellular internalization. The positively charged nanoparticles showed significantly much more internalization by Caco-2 cells ($P < 0.05$), suggesting that surface charge played an important role in cellular uptake of CMC–QC nanoparticles (Kumar et al., 2008). The results here from flow cytometry were in accordance with those observed by confocal microscopy. It's worthwhile to note that the negatively charged protein-encapsulated nanoparticles also exhibited somewhat efficient cellular uptake as compared with free proteins, despite the unfavorable electrostatic repulsion interaction between the negatively charged nanoparticles and the cellular membrane. As well known, most of natural polysaccharides have hydrophilic groups such as hydroxyl, carboxyl and amino groups, which could form non-covalent bonds with biological tissues (Liu et al., 2008). Herein in our study, the cellulose polysaccharide coating of the nanoparticles would facilitate the adhesion of nanoparticles to the cell membrane due to the bio-adhesion properties (Lemarchand et al., 2006).

4. Conclusions

In this work, effect of surface charge on efficacy of cellulose nanoparticles for delivery of both positively and negatively charged proteins was investigated. EE and LC of negatively charged BSA in the positively charged nanoparticles was 67.7% and 54.2%, respectively. EE and LC of positively charged LYS in the negatively charged nanoparticles could reach to 85.1% and 60.8%, respectively. Proteins encapsulated in the optimal nanoparticles could be sustainably released, and no obvious protein denaturation was detected during the process of encapsulation or release. The negatively charged nanoparticles didn't exhibit obvious cytotoxicity owing to the negative surface charge; the positively charged nanoparticles showed low toxicity due to the cellulose biocompatibility.

The surface charge played an important role in cellular uptake of CMC–QC nanoparticles. The positively charged protein-encapsulated nanoparticles were more efficiently internalized because of the electrostatic interaction with negatively charged cell membrane; the negatively charged protein-encapsulated nanoparticles also exhibited somewhat efficient cellular internalization, might due to the biologically adhesive polysaccharide coating. Therefore theoretically, the positively charged CMC–QC nanoparticles could form the primary platform as delivery carriers and exhibit favorable efficacy in most therapy cases (Verma & Stellacci, 2010), such as anticancer therapy and gene therapy, because they can overcome cell membrane barrier quickly, thus increase the drug concentration at the target sites (Yue et al., 2011). On the other hand, the negatively charged CMC–QC nanoparticles with less cellular uptake might be more appropriate used for delivering drugs such as insulin, which need the longer half-life (Yue et al., 2011). Also the negatively charged CMC–QC nanoparticles, which diffuse more quickly, might perform better for delivering drugs deep into tissues (Kim et al., 2010).

Acknowledgments

The authors are grateful to the Natural Sciences and Engineering Research Council of Canada (NSERC), the Alberta Livestock and Meat Agency Ltd. (ALMA) and the Alberta Crop Industry Development Fund Ltd. (ACIDF) for financial support as well as Canada Foundation for Innovation (CFI) for equipment support. We thank Alberta-Pacific Forest Industries Inc. (Alberta) for providing wood cellulose. Lingyun Chen would like to thank the Natural Sciences and Engineering Research Council of Canada (NSERC)-Canada Research Chairs Program for its financial support.

References

Boddohi, S., Moore, N., Johnson, P. A., & Kipper, M. J. (2009). Polysaccharide-based polyelectrolyte complex nanoparticles from chitosan, heparin, and hyaluronan. *Biomacromolecules*, *10*, 1402–1409.

Bouillot, P., Ubrich, N., Sommer, F., Duc, T. M., Loeffler, J. P., & Dellacherie, E. (1999). Protein encapsulation in biodegradable amphiphilic microspheres. *International Journal of Pharmaceutics*, *181*, 159–172.

Cai, C., Bakowsky, U., Rytting, E., Schaper, A. K., & Kissel, T. (2008). Charged nanoparticles as protein delivery systems: a feasibility study using lysozyme as model protein. *European Journal of Pharmaceutics and Biopharmaceutics*, *69*, 31–42.

Chen, F., Zhang, Z. R., Yuan, F., Qin, X., Wang, M., & Huang, Y. (2008). In vitro and in vivo study of N-trimethyl chitosan nanoparticles for oral protein delivery. *International Journal of Pharmaceutics*, *349*, 226–233.

Chen, L., Remondetto, G., Rouabhia, M., & Subirade, M. (2008). Kinetics of the breakdown of cross-linked soy protein films for drug delivery. *Biomaterials*, *29*, 3750–3756.

Chen, Q., Hu, Y., Chen, Y., Jiang, X., & Yang, Y. (2005). Microstructure formation and property of chitosan-poly(acrylic acid) nanoparticles prepared by macromolecular complex. *Macromolecular Bioscience*, *5*, 993–1000.

des Rieux, A., Fievez, V., Garinot, M., Schneider, Y. J., & Préat, V. (2006). Nanoparticles as potential oral delivery systems of proteins and vaccines: A mechanistic approach. *Journal of Controlled Release*, *116*, 1–27.

Drogoz, A., David, L., Rochas, C., Domard, A., & Delair, T. (2007). Polyelectrolyte complexes from polysaccharides: formation and stoichiometry monitoring. *Langmuir*, *23*, 10950–10958.

Garnett, M. C., & Kallinteri, P. (2006). Nanomedicines and nanotoxicology: some physiological principles. *Occupational Medicine*, *56*, 307–311.

Harush-Frenkel, O., Rozentur, E., Benita, S., & Altschuler, Y. (2008). Surface charge of nanoparticles determines their endocytic and transcytotic pathway in polarized MDCK cells. *Biomacromolecules*, *9*, 435–443.

Jadhav, S. B., & Singhal, R. S. (2014). Pullulan-complexed α-amylase and glucosidase in alginate beads: Enhanced entrapment and stability. *Carbohydrate Polymers*, *105*, 49–56.

Kamel, S., Ali, N., Jahangir, K., Shah, S. M., & El-Gendy, A. A. (2008). Pharmaceutical significance of cellulose: A review. *eXPRESS Polymer Letters*, *2*, 758–778.

Kim, B., Han, G., Toley, B. J., Kim, C. K., Rotello, V. M., & Forbes, N. S. (2010). Tuning payload delivery in tumour cylindroids using gold nanoparticles. *Nature Nanotechnology*, *5*, 465–472.

Kumar, R., Roy, I., Ohulchanskyy, T. Y., Goswami, L. N., Bonoiu, A. C., Bergey, E. J., et al. (2008). Covalently dye-linked, surface-controlled, and bioconjugated organically modified silica nanoparticles as targeted probes for optical imaging. *ACS Nano*, *2*, 449–456.

Lemarchand, C., Gref, R., Passirani, C., Garcion, E., Petri, B., Müller, R., et al. (2006). Influence of polysaccharide coating on the interactions of nanoparticles with biological systems. *Biomaterials*, *27*, 108–118.

Li, Q., Xia, B., Branham, M., Ha, W., Wu, H., Peng, S., et al. (2011). Self-assembly of carboxymethyl konjac glucomannan-*g*-poly(ethylene glycol) and (α-cyclodextrin) to biocompatible hollow nanospheres for glucose oxidase encapsulation. *Carbohydrate Polymers*, *86*, 120–126.

Liu, Z., Jiao, Y., Wang, Y., Zhou, C., & Zhang, Z. (2008). Polysaccharides-based nanoparticles as drug delivery systems. *Advanced Drug Delivery Reviews*, *60*, 1650–1662.

Mahmoud, K. A., Mena, J. A., Male, K. B., Hrapovic, S., Kamen, A., & Luong, J. H. (2010). Effect of surface charge on the cellular uptake and cytotoxicity of fluorescent labeled cellulose nanocrystals. *ACS Applied Materials & Interfaces*, *2*, 2924–2932.

Mao, Z., Zhou, X., & Gao, C. (2013). Influence of structure and properties of colloidal biomaterials on cellular uptake and cell functions. *Biomaterials Science*, *1*, 896–911.

Mo, R., Jiang, T., Di, J., Tai, W., & Gu, Z. (2014). Emerging micro- and nanotechnology based synthetic approaches for insulin delivery. *Chemical Society Reviews*, *43*, 3595–3629.

Pan, Y., Li, Y. J., Zhao, H. Y., Zheng, J. M., Xu, H., Wei, G., et al. (2002). Bioadhesive polysaccharide in protein delivery system: Chitosan nanoparticles improve the intestinal absorption of insulin in vivo. *International Journal of Pharmaceutics*, *249*, 139–147.

Ramineni, S. K., Cunningham, L. L., Dziubla, T. D., & Puleo, D. A. (2013). Competing properties of mucoadhesive films designed for localized delivery of imiquimod. *Biomaterials Science*, *1*, 753–762.

Sæther, H. V., Holme, H. K., Maurstad, G., Smidsrød, O., & Stokke, B. T. (2008). Polyelectrolyte complex formation using alginate and chitosan. *Carbohydrate Polymers*, *74*, 813–821.

Sadeghi, A. M., Dorkoosh, F. A., Avadi, M. R., Weinhold, M., Bayat, A., Delie, F., et al. (2008). Permeation enhancer effect of chitosan and chitosan derivatives: comparison of formulations as soluble polymers and nanoparticulate systems on insulin absorption in Caco-2 cells. *European Journal of Pharmaceutics and Biopharmaceutics*, *70*, 270–278.

Sandri, G., Bonferoni, M. C., Rossi, S., Ferrari, F., Gibin, S., Zambito, Y., et al. (2007). Nanoparticles based on N-trimethylchitosan: Evaluation of absorption properties using in vitro (Caco-2 cells) and ex vivo (excised rat jejunum) models. *European Journal of Pharmaceutics and Biopharmaceutics*, *65*, 68–77.

Sarmento, B., Ribeiro, A., Veiga, F., Sampaio, P., Neufeld, R., & Ferreira, D. (2007). Alginate/chitosan nanoparticles are effective for oral insulin delivery. *Pharmaceutical Research*, *24*, 2198–2206.

Schatz, C., Domard, A., Viton, C., Pichot, C., & Delair, T. (2004). Versatile and efficient formation of colloids of biopolymer-based polyelectrolyte complexes. *Biomacromolecules*, *5*, 1882–1892.

Song, Y., Gan, W., Li, Q., Guo, Y., Zhou, J., & Zhang, L. (2011). Alkaline hydrolysis and flocculation properties of acrylamide-modified cellulose polyelectrolytes. *Carbohydrate Polymers*, *86*, 171–176.

Song, Y., Wang, H., Zeng, X., Sun, Y., Zhang, X., Zhou, J., et al. (2010). Effect of molecular weight and degree of substitution of quaternized cellulose on the efficiency of gene transfection. *Bioconjugate Chemistry*, *21*, 1271–1279.

Song, Y., Zhou, J., Li, Q., Guo, Y., & Zhang, L. (2008). Preparation and characterization of novel quaternized cellulose nanoparticles as protein carriers. *Macromolecular Bioscience*, *9*, 863–867.

Song, Y., Zhou, Y., & Chen, L. (2012). Wood cellulose-based polyelectrolyte complex nanoparticles as protein carriers. *Journal of Materials Chemistry*, *22*, 2512–2519.

Song, Y., Zhou, Y., van Drunen Littel-van den Hurk, S., & Chen, L. (2014). Cellulose-based polyelectrolyte complex nanoparticles for DNA vaccine delivery. *Biomaterials Science*, *2*, 1440–1449.

Thanou, M. M., Kotzé, A. F., Scharringhausen, T., Luessen, H. L., de Boer, A. G., Verhoef, J. C., et al. (2000). Effect of degree of quaternization of N-trimethyl chitosan chloride for enhanced transport of hydrophilic compounds across intestinal caco-2 cell monolayers. *Journal of Controlled Release*, *64*, 15–25.

Win, K. Y., & Feng, S. S. (2005). Effects of particle size and surface coating on cellular uptake of polymeric nanoparticles for oral delivery of anticancer drugs. *Biomaterials*, *26*, 2713–2722.

van de Weert, M., Hoechstetter, J., Hennink, W. E., & Crommelin, D. J. (2000). The effect of a water/organic solvent interface on the structural stability of lysozyme. *Journal of Controlled Release*, *68*, 351–359.

Verma, A., & Stellacci, F. (2010). Effect of surface properties on nanoparticle-cell interactions. *Small*, *6*, 12–21.

Yeo, Y., & Park, K. (2004). Control of encapsulation efficiency and initial burst in polymeric microparticle systems. *Archives of Pharmacal Research*, *27*, 1–12.

Yue, Z., Wei, W., Lv, P., Yue, H., Wang, L., Su, Z., et al. (2011). Surface charge affects cellular uptake and intracellular trafficking of chitosan-based nanoparticles. *Biomacromolecules*, *12*, 2440–2446.

Zhang, J., Field, C. J., Vine, D., & Chen, L. (2014). Intestinal uptake and transport of vitamin b12-loaded soy protein nanoparticles. *Pharmaceutical Research*, http://dx.doi.org/10.1007/s11095-014-1533-x